Received: 30 August 2021 | Revised: 7 December 2021 | Accepted: 28 December 2021

DOI: 10.4218/etrij.2021-0284

ORIGINAL ARTICLE

ETRI Journal WILEY

Electroabsorption modulator-integrated distributed Bragg reflector laser diode for C-band WDM-based networks

Oh-Kee Kwon | **Chul-Wook Lee** | **Ki-Soo Kim**

Photonic Convergence Components Research Group, Electronics and Telecommunications Research Institute, Daejeon, Republic of Korea

Correspondence
Oh-Kee Kwon, Photonic Convergence Components Research Group, Electronics and Telecommunications Research Institute, Daejeon, Republic of Korea.
Email: okkwon@etri.re.kr

Funding information
Electronics and Telecommunication Research Institute Grant, Grant/Award Number: 21YB1810/ 21EB1210; ICT R&D program MSIP/IITP, Grant/Award Number: 2020-0-00847; Korea Innovation Foundation, Grant/Award Number: 2021-DD-RD-0082

Abstract

We report an electroabsorption modulator (EAM)-integrated distributed Bragg reflector laser diode (DBR-LD) capable of supporting a high data rate and a wide wavelength tuning. The DBR-LD contains two tuning elements, plasma and heater tunings, both of which are implemented in the DBR section, which have blue-shift and red-shift in the Bragg wavelength through a current injection, respectively. The light created from the DBR-LD is intensity-modulated through the EAM voltage, which is integrated monolithically with the DBR-LD using a butt–joint coupling method. The fabricated chip shows a threshold current of approximately 8 mA, tuning range of greater than 30 nm, and static extinction ratio of higher than 20 dB while maintaining a side mode suppression ratio of greater than 40 dB under a window of 1550 nm. To evaluate its modulation properties, the chip was bonded onto a mount including a radio-frequency line and a load resistor showing clear eye openings at data rates of 25 Gb/s nonreturn-to-zero and 50 Gb/s pulse amplitude modulation 4-level, respectively.

KEYWORDS
25 Gb/s NRZ, 50 Gb/s PAM-4, distributed Bragg reflector laser diode, electroabsorption modulator, wavelength division multiplexing, wavelength tuning

1 | INTRODUCTION

Tunable lasers are required for various applications, such as fiber-optic communication, optical precision measurements, optical sensing, bio-optics, and environmental gas detection. In particular, as colorless high-speed light sources, tunable optical transmitters operating at a 10 Gb/s data rate and higher for each wavelength channel in a wavelength division multiplexing (WDM) system are the core components of the next-generation broadband backhaul, data center, and radio access networks [1–3].

The use of tunable transmitters in the C-band [4–6] and O-band [7–9] has been demonstrated. A distributed Bragg reflector laser diode (DBR-LD) with a single grating mirror has been considered a promising light source for point-to-point WDM-based networks due to its compact size, simple operation, low cost, and good long-term reliability. In addition, its tuning range has been significantly enhanced to as wide as 26 nm for the C-band by applying two tuning elements [6] and more than 15 nm for the O-band by applying heater tuning (HT) only [8].

However, the excess signal chirp of directly modulated lasers at above 10 Gb/s has been a critical factor limiting the transmission distance under a C/L-band operation and can be overcome using a chirp-managed laser [10], electrical precompensations [11,12], an effect of adiabatic chirp [13], and an external modulator [1,14–20]. Among them, electroabsorption modulators (EAMs) using the quantum-confined Stark effect have been widely used due to a lower driving voltage, better electro-optic linearity, larger modulation bandwidth, and smaller chirp.

We recently developed an EAM-integrated DBR-LD for the O-band operation and demonstrated a 16-channel operation at a data rate of 25 Gb/s nonreturn-to-zero (NRZ) per channel [20]. In this study, we propose a structure capable of operating in the C-band and supporting improved performance in terms of the tuning range and data rate as well as evaluate the static properties of fabricated chips and dynamic properties of modules under various operational conditions. The rest of this article is organized as follows. The proposed device structure and its fabrication are described in Section 2. Section 3 presents the experimental results for the C-band EAM-integrated DBR-LDs. Finally, Section 4 concludes this study.

2 | DEVICE STRUCTURE

Figure 1 shows a schematic layer structure of the EAM-integrated DBR-LD. The device comprises gain, phase control (PC), DBR, and EAM sections. The light generated from the resonance cavity (i.e., DBR-LD, gain to DBR section) is intensity-modulated by the EAM and output from the antireflection facet. The total length of

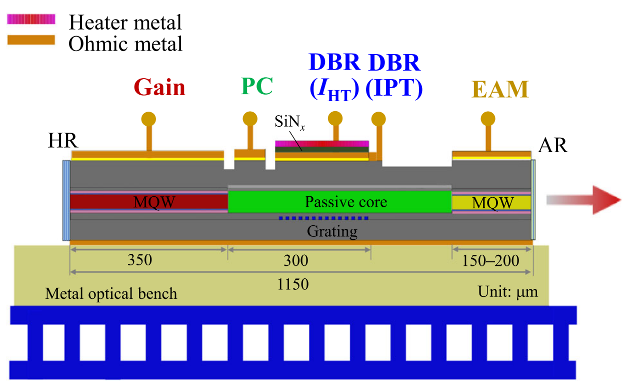

FIGURE 1 A schematic layer structure of the electroabsorption modulator (EAM)-integrated distributed Bragg reflector laser diode (DBR-LD). The front facet is anti-reflection (AR)-coated with a remaining power reflectivity of less than 0.1%, and the rear facet is high-reflection (HR)-coated, where I_{PT} and I_{HT} denote the current used for PT and HT, respectively

the fabricated chips is 1.15 mm, for which the lengths of the DBR-LD and EAM are designed to be 650 and 150 μm –200 μm, respectively.

In this structure, the lasing wavelength was tuned through carrier injection into a passive core through an ohmic metal in the DBR section, plasma tuning (PT), Joule heating of the waveguide using a thin-film metal, and HT, which shift the Bragg wavelength through a refractive index change of the DBR section according to Bragg's law (i.e., $\lambda_B = 2\Lambda n_{eq}$, where λ_B, Λ, and n_{eq} are the Bragg wavelength, grating period, and equivalent refractive index of the DBR section, respectively). Each metal is electrically isolated by inserting a dielectric SiN_x layer between them, which enables an independent tuning operation.

The overall fabrication process is nearly the same as in Kwon and others [20], except for the structure of grating, bandgap of the epitaxial layers, and metallization process of the DBR section. To allow the LD to operate within the C-band, the grating was designed to have a Bragg wavelength of approximately 1.55 μm and a coupling coefficient of approximately 25 cm^{-1}. Specifically, a 200-μm-long grating layer has a 25-nm-thick n-doped InGaAsP material (doping concentration $\cong$ 1×10^{18} cm^{-3} and bandgap wavelength $\cong$1.3 μm), and its period and duty are 240 nm and 0.35, respectively. For the designed structure, the power reflectivity of approximately 0.2 was obtained according to the coupled wave equation [21].

As for the epitaxial layers for the C-band operation, the multiple quantum wells (MQWs) and separate heterostructure (SCH) layers of the gain section were designed to have an optical gain near a 1.55-μm wavelength and those of the EAM to have a detuning of approximately 60 nm from the gain peak wavelength. Details for the layer structures are summarized in Table 1. After the growing processes, photo-luminescent (PL) measurements were taken (Figure 2). The peak wavelengths in terms of the gain and EAM sections obtained were approximately 1.55 μm and 1.49 μm, respectively.

In a monolithically integrated waveguide structure, the DBR-LD, including the gain, PC, and DBR sections, was fabricated into an etched-mesa buried SCH (EMBH) with a 12-μm width, and the EAM was fabricated into a deep ridge waveguide (DRWG) with a 2.5-μm width. After the formation of the waveguide, a benzocyclobutene (BCB) island was implemented next to the waveguide of the EAM section, a Ti/Pt/Au electrode was then formed as the p-type ohmic contact, and a Cr/Au electrode was used as the heating metal. The width and length of the heating metal were designed to be 4 and 200 μm, respectively, and the resistance obtained was approximately 80 Ω. Figure 3 shows the scanning

TABLE 1 Epitaxial layers of gain, passive, and EAM sections

Section	Structure	InGaAsP material thickness, bandgap wavelength, and strain
Gain	7 QWs	
	- 7 wells	6 nm, 1.68 μm, and compressive 0.8%
	- 8 barriers	8 nm, 1.24 μm, and tensile 0.6%
	- Inner SCH	30 nm, 1.24 μm, and lattice-matched
	- Outer SCH	50 nm, 1.08 μm, and lattice-matched
Passive core	Bulk	0.27 μm, 1.3 μm, and lattice-matched
EAM	10 QWs	
	- 10 wells	8.5 nm, 1.55 μm, and compressive 0.5%
	- 11 barriers	6 nm, 1.24 μm, and tensile 0.4%
	- SCH	70 nm, 1.24 μm, and lattice-matched

Abbreviations: EAM, electroabsorption modulator; SCH, separate hetero-structure; QW, quantum well.

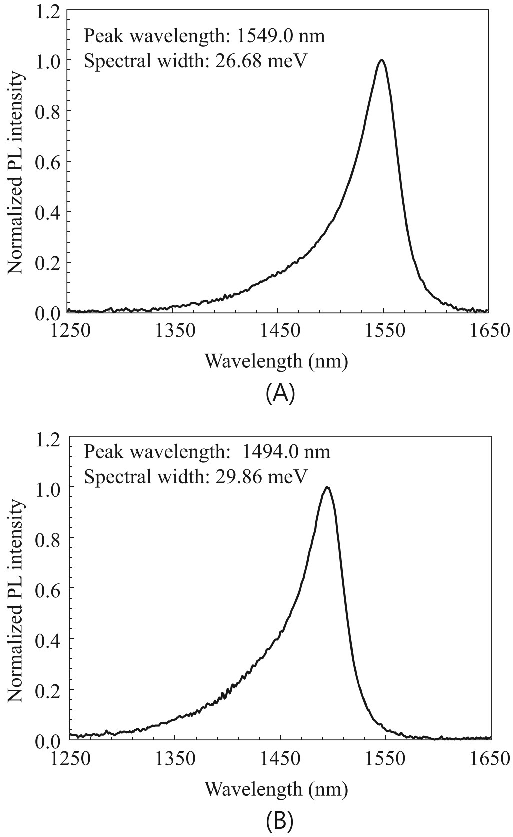

FIGURE 2 Photo-luminescent (PL) spectra of multiple quantum wells (MQWs) grown in (A) the gain and (B) the electroabsorption modulator (EAM) sections. The wavelength detuning obtained between the MQWs of the gain and EAM is 55 nm

electron microscopy (SEM) images of the (A) fabricated chip and cross-sectional views of the (B) gain and (C) EAM sections.

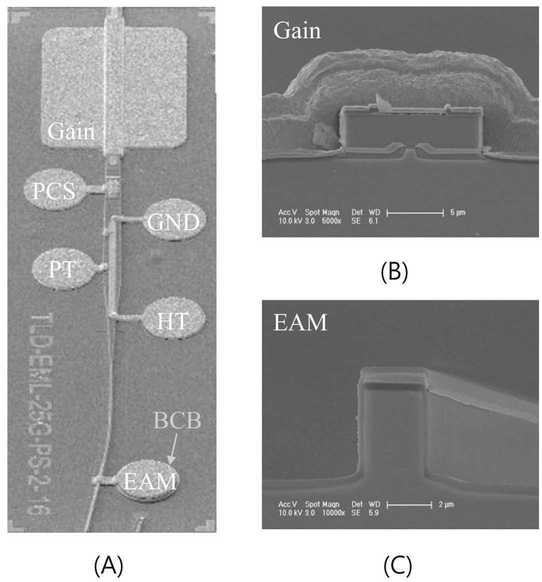

FIGURE 3 Scanning electron microscopy (SEM) images of the (A) fabricated chip and cross-sections of the (B) gain and (C) electroabsorption modulator (EAM) sections. In (A), the output waveguide is tilted 9°

After the scribing and facet coatings, the static properties were tested, and the chip was bonded onto a metal optical bench (MOB) with a radiofrequency (RF) line and 50-Ω load (Figure 4).

3 | RESULTS AND DISCUSSION

Figure 5A shows typical light versus gain current (L–I) characteristics of the chips with an EAM length L_{EAM} of 180 μm at an operating temperature of 25°C. The

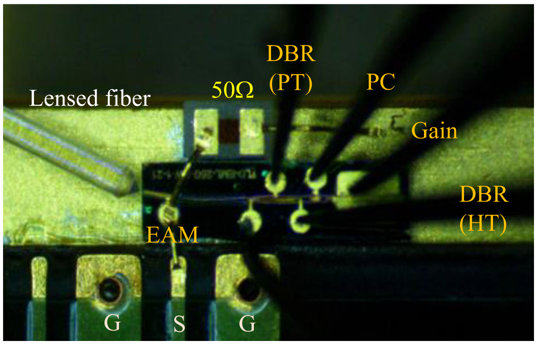

FIGURE 4 Photograph of distributed Bragg reflector laser diode (DBR-LD) chip electroabsorption modulator (EAM)-integrated onto a metal optical bench (MOB) with a ground-signal-ground (GSG) radiofrequency (RF) line and a 50-Ω load

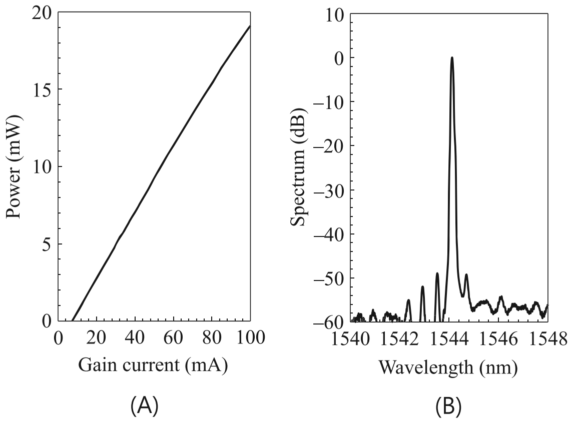

FIGURE 5 (A) L–I characteristics of 180-μm-long electroabsorption modulator (EAM)-integrated distributed Bragg reflector laser diodes (DBR-LDs) and (B) output spectrum at an 80-mA gain current

threshold current and slope efficiency appeared to be within a range of approximately 8 mA and 0.2 W/A, respectively, and the output power obtained was 19 mW at a current of 100 mA. Figure 4B shows the output spectrum at a current of 80 mA; its peak wavelength was approximately 1544 nm, and the side mode suppression ratio (SMSR) was as high as 50 dB.

For a tuning operation with the currents in the DBR-LD, it is well-known that the PT and HT shift the Bragg wavelength to the shorter and longer wavelength sides, respectively. To confirm the validity of their operation for this integrated structure, we measured the peak wavelength of the output spectrum as a function of the currents, I_{PT} and I_{HT}. As shown in Figure 6, both trajectories appear nearly similar to those in Kwon and others [6], and the total tuning range exceeds 30 nm within the range of the operating current.

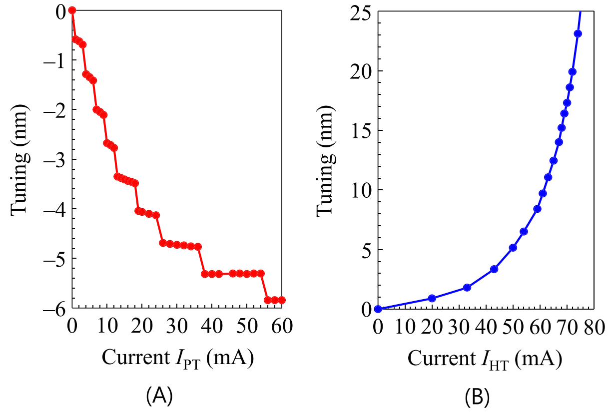

FIGURE 6 Wavelength tuning with respect to (A) the current for plasma tuning (PT) I_{PT} and (B) the current for heater tuning (HT) I_{HT} for electroabsorption modulator (EAM)-integrated distributed Bragg reflector laser diode (DBR-LD). The tuning range of I_{HT} is about four times larger than that of I_{PT} within the range of the operating current

Moreover, the mode jump, the interval of which corresponds to the free spectral range of the DBR-LD, $\Delta\lambda_{FSR}$, is shown clearly in the PT curve, although found in both tuning curves. With this structure, the lasing wavelength was fine-tuned through the use of a PC current I_{PC}, making λ_{peak} to move within the range of $\pm\Delta\lambda_{FSR}/2$.

Figure 7 shows superimposed tuning spectra with different tuning currents at an 80-mA gain current, indicating a power loss of <3 dB and SMSR of >45 dB, with a wavelength range of approximately 20 nm (i.e., 1539 nm–1559 nm). Notably, the maximum value in peak power appears at a 1546-nm wavelength (red line) and not at 1544 nm (black, reference wavelength), and the power reduction during the HT operation was significantly smaller than that of the PT. For the red-shift in the maximum peak power and the salient asymmetry in the power reduction, apart from the optical losses due to the tuning operation itself (i.e., free-carrier loss for the electron and holes, thermal loss, and other factors), we believe it might originate mainly from the EAM absorption, the peak wavelength of which was positioned at approximately 1490 nm, making a shorter wavelength experience a higher optical loss.

To examine the modulation property of the EAM section, the fabricated chip was bonded onto the MOB, and its output power was measured with the voltage applied to the EAM section. Figure 8 shows the extinction ratio (ER), the value normalized by the power obtained at zero voltage, for modules with an EAM length L_{EAM} of 180 μm or 200 μm. The ER has a reverse sigmoid shape with the EAM voltage. As L_{EAM} increases, ER quickly fell off with the voltage; consequently, an ER of −10 dB is

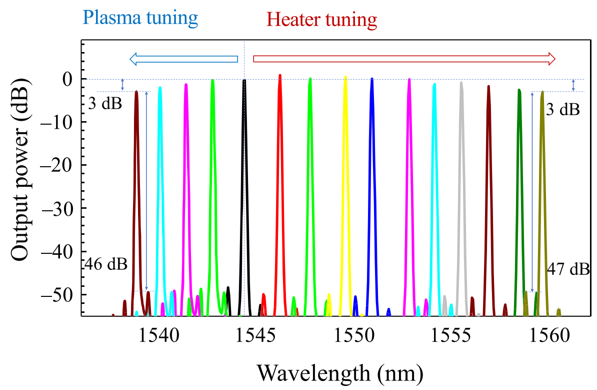

FIGURE 7 Superimposed tuning spectra of a fabricated laser diode (LD) chip with different tuning currents. During this measurement, the gain current is fixed at 80 mA, and I_{PT} and I_{HT} are varied within a range of 0–50 mA and 0–70 mA, respectively

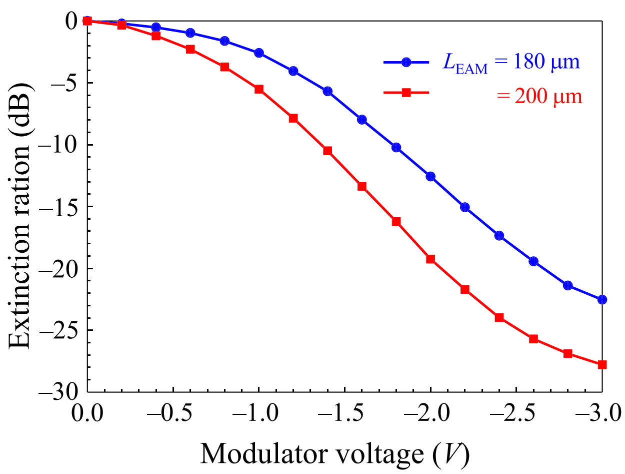

FIGURE 8 Extinction ratio (ER) with respect to electroabsorption modulator (EAM) voltage at the reference wavelength for an laser diode (LD) module with 180-μm-long (blue) and 200-μm-long (red) EAMs

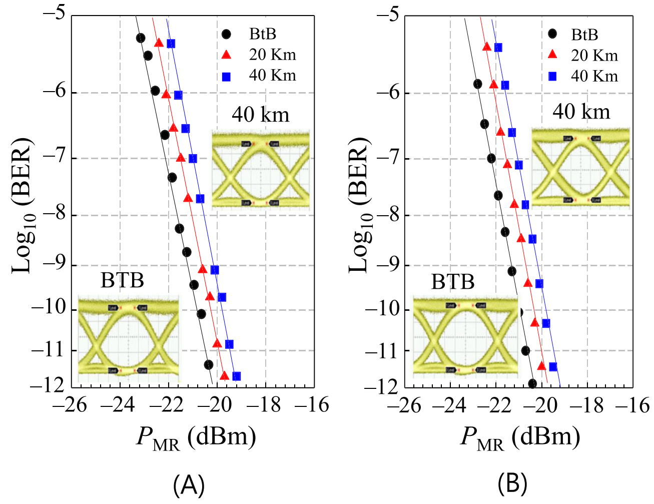

FIGURE 9 Bit error rate (BER) performances of 10 (10.3125) Gb/s NRZ signal at the BtB (black) and after 20-km (red) and 40-km (blue) transmissions with respect to P_{MR} at wavelengths of (A) 1539 nm and (B) 1555 nm. Inlets show the measured optical eye diagrams before and after 40-km transmission at respective wavelengths

obtained at −1.8 V and −1.4 V for the L_{EAM} of 180 μm and 200 μm, respectively. However, it is extremely crucial to select a proper L_{EAM} satisfying the required data rate because the modulation bandwidth depends highly on L_{EAM} according to the junction capacitance model [22]. After testing the electro-optic response for the modules, we confirmed that they had a −3-dB bandwidth of more than 14 GHz for the L_{EAM} of 200 μm and 20 GHz for the L_{EAM} of 180 μm.

The large-signal modulation and the transmission were performed for a 10 Gb/s NRZ signal with a pseudo-random bit sequence of 2^{31}–1 with the 200-μm-long EAM-integrated LD module. In this test, the gain current I_{gain} was fixed to be 80 mA. Figure 9A,B shows the bit error rate (BER) link performance through single-mode fiber transmissions with respect to the minimum received power P_{MR} at a wavelength of 1539 nm and 1555 nm, respectively. An EAM voltage V_{EAM} of −1.2 V and a peak-to-peak voltage V_{pp} of 2.5 V were applied for both wavelengths. The eye patterns were opened before and after a 40-km transmission at both operating wavelengths; consequently, power penalties of less than 1 dB were achieved. Moreover, as the wavelength moved to the shorter wavelength side, an eye cross-point tended to be lowered due to the change of ER curve with respect to the tuning wavelength. Consequently, it is desirable to adjust the V_{EAM} to the operating wavelength.

Using the module with a 180-μm-long EAM section, an optical eye diagram test was performed for the 25 Gb/s NRZ and 50 Gb/s pulse amplitude modulation 4-level (PAM-4) signals. During this test, each DC was supplied to the chip pad through each single-tip probe (Figure 4), and the EAM voltage and the RF signal amplified by a single-ended linear amplifier (with an S21 bandwidth of 56 GHz) were combined by a bias tee and then applied to the EAM pad through a bonding wire from a GSG line (with an S21 bandwidth of >40 GHz). Figure 10 shows the measured optical eye patterns of the 25 Gb/s NRZ and 50 Gb/s PAM-4 signals for the BtB at the reference wavelength. During the measurement, V_{pp} and V_{EAM} were adjusted to obtain a dynamic ER of approximately 6 dB and an eye-crossing of 50% for the NRZ signal. For the PAM-4 signal, the voltage levels were additionally controlled to obtain an equally spaced eye height among the various levels (i.e., voltage ratio of the upper, middle,

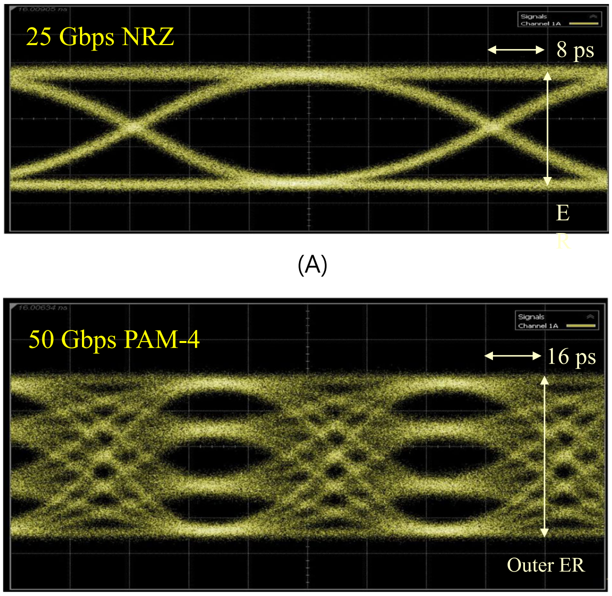

(A)

(B)

FIGURE 10 Optical eye pattern of (A) 25 (25.78125) Gb/s NRZ and (B) 50 (2 × 25.78125) Gb/s PAM-4 signal at the reference wavelength. In (A) and (B), V_{pp} and V_{EAM} are 2 V and −1.8 V, respectively. The extinction ratio (ER) in (A) and outer ER in (B) are obtained at approximately 6.5 dB and 6.1 dB, respectively

and lower eyes = 38%, 32%, and 30%, respectively) without any other pre-emphasis technique applied.

Regarding the effect of the wavelength tuning on the signal quality, when the PT current increased (i.e., the wavelength was blue-shifted) under a certain optimal condition, the ER increased, the eye-crossing point lowered for the NRZ signal, and the height of the upper eye increased for the PAM-4 signal. The HT operation yields an opposite outcome. Overall, a variation of approximately 2 dB in the ER under the same V_{pp} appeared over the range of 1539 nm to 1559 nm, which could be corrected more or less by simultaneously adjusting V_{EAM} and V_{pp}. By contrast, compared with the NRZ signal, the PAM-4 signal was highly sensitive to V_{EAM} and V_{pp} because of the limited linearity of the ER with the EAM voltage. Additional experimental results and their examinations for the PAM-4 signal will be submitted elsewhere.

4 | CONCLUSION

We developed an EAM-integrated DBR-LD supporting a wide tuning range within the C-band and a high data rate per wavelength. The epitaxial layers were designed for the DBR-LD's gain peak and EAM's absorption peak, appearing at wavelengths of 1.55 μm and 1.49 μm, respectively. Two tuning elements, PT and HT, were introduced within the DBR section for extending the tuning range. The DBR-LD was fabricated using an EMBH for a low operating current, and the EAM was fabricated using the DRWG with BCB islands for high-speed modulation. For the fabricated LDs with a 180-μm-long EAM, an output power of ∼20 mW and a total tuning range of more than 30 nm were obtained. A power loss of less than 3 dB and an SMSR of greater than 45 dB with a wavelength range of approximately 20 nm were shown. We also confirmed that the tuning operation of this integrated LD is nearly the same as that of a solitary DBR-LD due to the sufficiently low residual reflection from the output facet; in addition, the light at the shorter wavelength side could have a higher loss due to the EAM absorption. Through a dynamic test, two modules with different EAM lengths were investigated within a wavelength range of 1539 nm to 1555 nm. The 200-μm-long EAM-integrated DBR-LD with a −3-dB bandwidth of 14 GHz showed clear eye patterns for the 10 Gb/s NRZ signal, and the 180-μm-long EAM-integrated DBR-LD with a −3-dB bandwidth of 20 GHz showed clear eye patterns for both 25 Gb/s NRZ and 50 Gb/s PAM-4 signals. Based on the results, we conclude that the EAM-integrated DBR-LD can be used as an effective light source for C-band WDM-based networks, such as dense WDM, cable television, and interdata-center applications.

FUNDING INFORMATION

This work was supported by the Korea Innovation Foundation funded by Korea Government (MSIT) (no. 2021-DD-RD-0082, Commercialization of 8 wavelength DBR-EAM chip with modulation rate of 25 Gb/s per channel), the ICT R&D program MSIP/IITP (no. 2020-0-00847, Development of 5G+ mobile fronthaul transport technology), and the Electronics and Telecommunication Research Institute Grant funded by the Korea Government (no. 21YB1810/21EB1210, Development of DBR-EAM LD chip technology for commercialization).

CONFLICT OF INTEREST

The authors declare that there are no conflict of interest related to this article.

ORCID

Oh-Kee Kwon https://orcid.org/0000-0002-2065-2191

REFERENCES

1. J. Shin, S. Hong, J. Y. Lim, S. Cho, H. Y. Rhy, and G. Y. Yi, *CWDM network with dual sub-channel interface for mobile fronthaul and backhaul deployment*, (16th International Conference on Advanced Communication Technology, Pyeongchang, Rep. of Korea), Feb. 2014, pp. 1009–1102.

2. J. Zhu, A. Wonfor, S. H. Lee, S. Pachnicke, M. Lawin, R. V. Penty, J. P. Elbers, R. Cush, M. J. Wale, and I. H. White, *Athermal colorless C-band optical transmitter system for passive optical networks*, J. Lightwave Technol. **32** (2014), no. 22, 4253–4260.
3. I. A. Alimi, A. L. Teixeira, and P. P. Monterio, *Toward an efficient C-RAN optical fronthaul for the future networks: A tutorial on technologies requirements, challenges, and solutions*, IEEE Commun. Surv. Tutorials **20** (2018), no. 1, 708–769.
4. B. S. Choi, S. H. Oh, K. S. Kim, K. H. Yoon, H. S. Kim, M. R. Park, J. S. Jeong, O. K. Kwon, J. K. Seo, H. K. Lee, and Y. C. Chung, *10-Gb/s direct modulation of polymer-based tunable external cavity lasers*, Opt. Express **20** (2012), no. 18, 20368–20375.
5. D. Zhou, S. Liang, L. Zhao, H. Zhu, and W. Wang, *High-speed directly modulated widely tunable two-section InGaAlAs DBR lasers*, Opt. Express **25** (2017), no. 3, 2341–2346.
6. O. K. Kwon, C. W. Lee, K. S. Kim, S. H. Oh, and Y. A. Leem, *Proposal of novel structure for wide wavelength tunable in distributed bragg reflector laser diode with single grating mirror*, Opt. Express **26** (2018), no. 22, 28704–28712.
7. M. Yamaguchi, M. Kitamura, S. Murata, I. Mito, and K. Kobayashi, *Wide range wavelength tuning in 1.3 μm DBR-DC-PBH-LDs by current injection into the DBR region*, Electron. Lett. **21** (1985), no. 2, 63–65.
8. S. H. Oh, O. K. Kwon, K. S. Kim, and C. W. Lee, *1.3-μm and 10-Gb/s tunable DBR-LD for low-cost application of WDM-based mobile front haul networks*, Opt. Express **27** (2019), no. 20, 29241–29247.
9. T. Shindo, N. Fujiwara, Y. Ohiso, T. Sato, and H. Matsuzaki, *Quasi-continuous tuning of a 1.3-μm-wavelength superstructure grating distributed bragg reflector laser by enhancing carrier-induced refractive index change*, Opt. Express **29** (2021), no. 1, 232–243.
10. Y. Matsui, D. Mahgerefteh, X. Zheng, C. Liao, Z. F. Fan, K. McCallion, and P. Tayebati, *Chirp-managed directly modulated laser (CML)*, IEEE Photon. Technol. Lett. **18** (2006), no. 2, 385–387.
11. A. S. Kara, J. C. Cartledge, J. Harley, and K. Roberts, *Electronic pre-compensation for 10.7Gb/s system employing a directly modulated laser*, J. Lightwave Technol. **29** (2011), no. 13, 2069–2076.
12. K. Kwon, J. Yoon, and H. M. Bae, *A 6 Gb/s transceiver with a nonlinear electronic dispersion compensator for directly modulated distributed-feedback lasers*, IEEE J. Solid-State Circuits **50** (2015), no. 2, 503–514.
13. O. K. Kwon, H. S. Cho, C. W. Lee, S. H. Oh, Y. A. Leem, and E. S. Nam, *10-Gb/s 1.59-μm DFB-LD transmission over 20 km SMF with no compensation*, IEEE Photon Technol. Lett. **28** (2016), no. 4, 509–512.
14. O. K. Kwon, Y. S. Baek, and Y. C. Chung, *Electroabsorption modulated laser with high immunity to residual facet reflection*, IEEE J. Quantum Electron. **48** (2012), no. 9, 1203–1213.
15. O. K. Kwon, Y. S. Baek, Y. C. Chung, and H. M. Park, *Proposal and analysis of distributed reflector-laser diode integrated with an electroabsorption modulator*, ETRI J. **35** (2013), no. 3, 459–468.
16. L. Han, S. Liang, H. Wang, L. Qiao, J. Xu, L. Zhao, H. Zhu, B. Wang, and W. Wang, *Electroabsorption-modulated widely tunable DBR laser transmitter for WDM-PONs*, Opt. Express **22** (2014), no. 24, 30368–30376.
17. N. Eiselt, J. Wei, H. Griesser, A. Dochhan, M. H. Eiselt, J. Elbers, J. J. V. Olmos, and I. T. Monroy, *Evaluation of real-time 8×56.25 Gb/s (400G) PAM-4 for inter-data center application over 80 km of SSMF at 1550 nm*, J. Lightwave Technol. **35** (2017), no. 4, 955–962.
18. J. H. Lee, S. H. Chang, J. Y. Huh, S. K. Kang, K. Kim, and J. K. Lee, *EML based real-time 112Gbit/s (2 × 56.25 Gbit/s) PAM-4 signal transmission in C-band over 80 km SSMF for inter DCI applications*, Opt. Fiber Technol. **45** (2018), 141–145.
19. M. Y. Park, B. W. Kim, M. Moehrle, U. Troppenz, W. Rehbein, A. Sigmund, and S. J. Hong, *Liquid crystal filter based tunable transmitter for 25Gps wavelength division multiplexing-passive optical network fronthaul*, Opt. Express **28** (2020), no. 26, 38942–38948.
20. O. K. Kwon, C. W. Lee, S. H. Oh, and K. S. Kim, *16-channel tunable and 25-Gb/s EAM-integrated DBR-LD for WDM-based mobile front-haul networks*, Opt. Express **29** (2021), no. 2, 1805–1812.
21. H. Ghafouri-Shiraz, *Distributed Feedback Laser Diodes and Optical Tunable Filters*, John Wiley & Sons Ltd, England, 2003.
22. O. K. Kwon, Y. T. Han, Y. S. Baek, and Y. C. Chung, *Improvement of Modulation Bandwidth in Electroabsorption-Modulated Laser by Utilizing the Resonance Property in Bonding Wire*, Opt. Express **20** (2012), no. 11, 11806–11812.

AUTHOR BIOGRAPHIES

Oh-Kee Kwon received his PhD degree in Electronics Engineering form the Korea Advanced Institute of Science and Technology, Deajeon, Rep. of Korea, in 2012. Since 2002, he has been with Electronics and Telecommunications Research Institute, Daejeon, Rep. of Korea, where he is currently a principal research engineer. His current research interests are the dynamic single-mode lasers with high modulation speed and broad wavelength tunability and their arrayed structure based on the monolithic integration with the multiwavelength operation for optical communications and image systems.

Chul-Wook Lee received the BS, MS, and PhD degrees in Physics from Yeungnam University, Daegu, Rep. of Korea, in 1990, 1992, and 1998. Since 2000, he has worked in Electronics and Telecommunications Research Institute, Daejeon, Rep. of Korea, as a Member of the Research Staff. His main interests are the fabrication of semiconductor laser diodes and other optical devices for optical communications

Ki-Soo Kim received his BS and MS and PhD degrees in the Department of Physics and Semiconductor Science and Technology from Jeonbuk National University, Jeonju, Rep. of Korea, in 1995, 1997, and 2000, respectively. From 2000 to 2001, he worked at the Microelectronics Research Center of the University of Texas at Austin as a postdoctoral fellow. Since October 2001, he has been with the Electronics and Telecommunications Research Institute, Daejeon, Republic of Korea, as a principal member researcher. His research interests include photonic and optoelectronic semiconductor devices for telecommunication and sensor applications.

How to cite this article: O.-K. Kwon, C.-W. Lee, and K.-S. Kim, *Electroabsorption modulator-integrated distributed Bragg reflector laser diode for C-band WDM-based networks*, ETRI Journal **45** (2023), 163–170. https://doi.org/10.4218/etrij.2021-0284